Journal of the Iranian Chemical Society (2021) 18:225–232
https://doi.org/10.1007/s13738-020-02021-x

ORIGINAL PAPER

The synthesis and dielectric properties of a new phenylbenzoate-based calamitic liquid crystal

Esma Ahlatcıoğlu Özerol[1] · Hale Ocak[2] · Belkız Bilgin Eran[2] · Selvi Karavelioğlu[2]

Received: 29 April 2020 / Accepted: 24 July 2020 / Published online: 4 August 2020

Abstract

The dielectric investigation has a great importance in liquid crystal studies as a supportive method to DSC for a complete characterization of liquid crystals as well as in the electronic applications. In this study, the synthesis, mesomorphic characterization and dielectric properties of a new phenylbenzoate-based three-ring calamitic liquid crystal which composed of ester linking groups, *(S)-3,7-dimethyloctyloxy* chiral unit at one of terminals and *n*-octyloxy chain at the other end of the molecule, have been reported. The new calamitic liquid crystal 4-[4-((*S*)-3,7-dimethyloctyloxy)phenoxy)carbonyl]phenyl 4-(*n*-octyloxy)benzoate (DPCPB) has been characterized using ^{1}H, ^{13}C-NMR and MS-QTOF. The liquid crystalline behavior of the target compound has been investigated by differential scanning calorimetry and optical polarizing microscopy. DPCPB exhibits an enantiotropic non-tilted smectic mesophase in a wide temperature range. The real and imaginary dielectric constant, conductivity mechanism, impedance and dielectric relaxation mechanism of DPCPB have been investigated depending on frequency at different temperatures.

Keywords Calamitic liquid crystal · *(S)-3,7-Dimethyloctyloxy* chiral unit · Smectic phase · Dielectric properties

Introduction

Liquid crystals (LCs) that are able to self-assembly are one of the most unique classes of soft materials [1, 2]. These materials combine both fluidity and long-range order properties which enable the more advanced applications of LC [3, 4], most prominently in various fields such as display technology [5, 6], electro-optics, fast switching devices [7, 8], organic light-emitting diodes (OLEDs) [9–12], biosensors [13–15], organic semiconductors [16] and nanoparticle-doped LCs-based devices [17, 18].

LC materials show a variety of mesophases depending on their molecular architecture and the intermolecular interactions which are responsible for the self-organization. The molecular shape and the interactions influence the macroscopic behavior and give rise to a considerable change in the mesomorphic properties. It is necessary to determine the appropriate molecular design and to understand more deeply the structure–property relations for new technological challenges [1, 2, 19].

Calamitic liquid crystals, which are the most studied class in the LC field, are generally composed of at least two aromatic rings linked each other directly or by a flexible connecting group and carry alkyl chains or polar groups at terminals of the structure. The alteration of terminal chains, connecting units and lateral substitution of the rigid core of a calamitic molecule is generally useful ways to change the molecular rigidity, flexibility and physical properties of LCs [2, 19–22]. Phenyl benzoate-based liquid crystals are one of the most synthesized molecular architecture due to the molecular flexibility arised from ester linking groups between aromatic rings, the advantages of easily synthesis methods as well as the alteration of lateral and terminal substitution possibility which enables the occurrence of unique physical properties [23–28].

Chiral liquid crystals (LCs) have gained much attention since the discovery of ferroelectric properties [29] which

Electronic supplementary material The online version of this article (https://doi.org/10.1007/s13738-020-02021-x) contains supplementary material, which is available to authorized users.

✉ Esma Ahlatcıoğlu Özerol
eahlatci@yildiz.edu.tr

[1] Department of Bioengineering, Yildiz Technical University, 34220 Istanbul, Turkey

[2] Department of Chemistry, Yildiz Technical University, 34220 Istanbul, Turkey

gave rise to the development of LC display technology [30, 31]. The molecular chirality can be introduced into various locations of the mesogenic unit [32]. In general, the chiral moieties are generally introduced as a terminal group into the structure. The variation of a mesogenic core by chiral centers leads to the chiral mesophases such as chiral smectics and cholesteric mesophase [33–38].

The investigation of dielectric behavior of liquid crystals is of significant interest to improve the physical properties of liquid crystal materials and the new design of smart multifunctional liquid crystalline materials aimed for optoelectronic applications [39–41]. The dielectric study is also necessary to understand the effect of nanoparticles on the improvement of the dielectric properties of nanoparticle-doped liquid crystal mixtures and to produce new LC-NP composite materials having unique and improved properties that are different from pure LCs for technological applications [42–44].

In this study, we reported the synthesis, mesomorphic characterization and dielectric properties of a new chiral calamitic liquid crystal DPCPB which is derived from the phenylbenzoate ester with three aromatic rings as the rigid unit, *(S)-3,7-dimethyloctyloxy* chiral unit at one of ends and *n*-octyloxy chain at the other. As a supportive method to DSC and POM techniques, the dielectric properties such as real and imaginary dielectric constant, conductivity mechanism, impedance and dielectric relaxation mechanism have been investigated depending on frequency at different temperatures in order to enable the determination of the phase transition temperatures of DPCPB.

Experimental

Synthesis and mesomorphic properties of 4-[4-((*S*)-3,7-dimethyloctyloxy)phenoxy) carbonyl]phenyl 4-(*n*-octyloxy)benzoate (*DPCPB*)

The synthesis of a new phenylbenzoate-based three-ring calamitic liquid crystal 4-[4-((*S*)-3,7-dimethyloctyloxy)phenoxy)carbonyl]phenyl 4-(*n*-octyloxy)benzoate (*DPCPB*) is carried out as shown in Scheme 1. Firstly, 4-(*n*-octyloxy) benzoic acid [45] (**2**) was synthesized by the etherification of commercially available *n*-octyl bromide with ethyl 4-hydroxybenzoate in 2-butanone using K_2CO_3 to yield ethyl 4-(*n*-octyloxy)*benzoate* [46] (**1**), followed by hydrolysis reaction with NaOH/H_2O in ethanol. The *(S)*-3,7-dimethyloctyloxy chain substituted phenol ring was synthesized by firstly starting reduction of (*S*)-(–)-β-citronellol to the saturated corresponding chiral alcohol under catalytic hydrogenation condition. Then, the bromination reaction with 48% aqueous HBr/concentrated H_2SO_4 using tetrabutylammonium hydrogensulfate (TBAHS) as catalyst was carried out to yield *(S)*-3,7-dimethyloctyl-1-bromide [47, 48]. The Williamson ether synthesis *of (S)*-3,7-dimethyloctyl-1-bromide and commercially available 4-benzyloxyphenol using K_2CO_3 in 2-butanone yield to *(S)-4-(3,7-dimethyloctyloxy) phenyl benzyl ether* [48] (**3**). The deprotection reaction of compound **3** using with 10% Pd/C as catalyst in THF by heating in autoclave under the pressure of H_2 gas yielded to *(S)-4-(3,7-dimethyloctyloxy)phenol* [49, 50] (**4**). The esterification of *(S)-4-(3,7-dimethyloctyloxy)phenol* (**4**) and *p*-benzyloxybenzoic acid [51] using *N,N'*-dicyclohexylcarbodiimide (DCC) and 4-(dimethylamino)pyridine (DMAP) [52] as catalyst in dry dichloromethane to afford *(S)-4-(3,7-Dimethyloctyloxy)phenyl 4-benzyloxybenzoate* [48] (**5**) followed by hydrogenolytic deprotection of the benzyl group leads to *(S)-4-(3,7-dimethyloctyloxy)phenyl 4-hydroxybenzoate* [48] (**6**). Finally, the esterification of 4-(*n*-octyloxy)benzoic acid (**2**) and *((S)-4-(3,7-dimethyloctyloxy)phenyl 4-hydroxybenzoate* (**6**) yielded to the target compound DPCPB (**7**) [53].

Procedure for the synthesis of 4-[4-((*S*)-3,7-dimethyloctyloxy)phenoxy) carbonyl]phenyl 4-(*n*-octyloxy)benzoate (*DPCPB*) (7)

4-(*n*-octyloxy)benzoic acid (**2**) (1.0 mmol) and *((S)-4-(3,7-dimethyloctyloxy)phenyl 4-hydroxybenzoate* (**6**) (1.1 mmol) were dissolved in dry CH_2Cl_2 (30 mL). To this solution, *N,N'*-dicyclohexylcarbodiimide (DCC) (1.25 mmol) and 4-(dimethylamino)pyridine (DMAP) (0.09 mmol) were added and the reaction mixture was stirred under argon atmosphere for 24 h at room temperature. The reaction was followed by TLC (hexane:ethyl acetate/2:1). The reaction mixture was filtered on silica gel with CH_2Cl_2, and solvent was removed under reduced pressure. The crude product was purified by column chromatography on silica gel, eluting with chloroform and then crystallization from a mixture of chloroform and ethanol.

The intermediates and DPCPB were characterized by ^{1}H-NMR and ^{13}C-NMR (Bruker Avance III 500 spectrometer in $CDCl_3$ or DMSO-d_6 solutions, with tetramethylsilane as internal standard). DPCPB was also characterized based on MS-QTOF (Agilent 6530, electrospray ionization, ion source: dual ESI, MS abs. threshold: 200, MS/MS abs. threshold: 5, gas flow rate: 10 L/min, gas temperature 300 °C) (see Figs. S3 and S4). The proposed structures are in full agreement with the obtained spectroscopic data.

4-[4-((*S*)-3,7-Dimethyloctyloxy)phenoxy)carbonyl] phenyl 4-(*n*-octyloxy)benzoate (*DPCPB*) (7)

$C_{38}H_{50}O_6$; 602.80 g/mol: **Yield:** 0.31 g (% 52), colorless crystals. **^{1}H NMR** (400 MHz, $CDCl_3$): δ (ppm) = 8.18 (*d*, $J \approx 8.8$ Hz; 2 Ar–H), 8.07 (*d*, $J \approx 8.9$ Hz; 2 Ar–H),

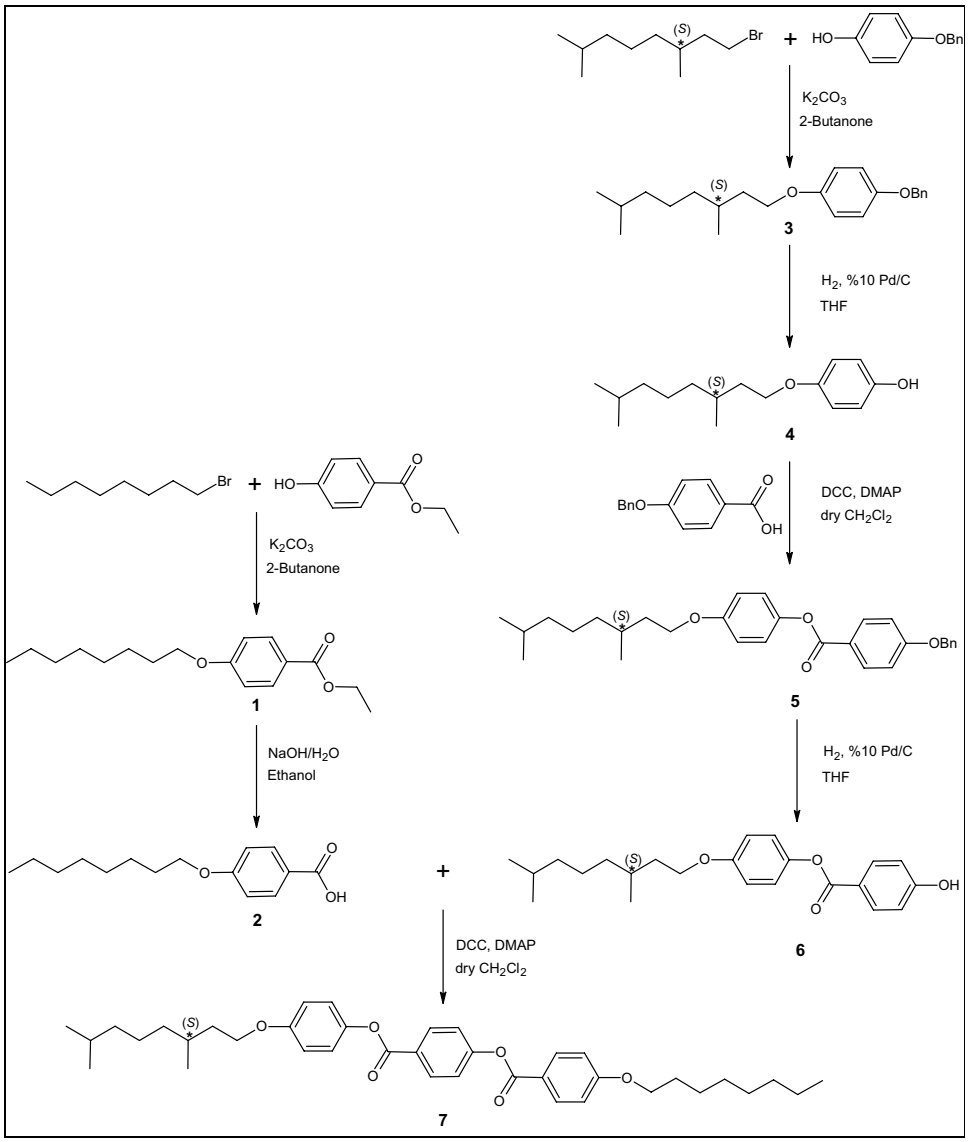

Scheme 1 The synthesis of a new phenylbenzoate-based three-ring calamitic liquid crystal *DPCPB*

7.27 (*d*, $J \approx 8.8$ Hz; 2 Ar–H), 7.04 (*d*, $J \approx 9.0$ Hz; 2 Ar–H), 6.90 (*d*, $J \approx 8.9$ Hz; 2 Ar–H), 6.85 (*d*, $J \approx 9.0$ Hz; 2 Ar–H), 3.95–3.87 (*m*; 4H, 2 OCH_2), 1.86–1.79, 1.77–1.44, 1.42–1.04 (3*m*; 22H, 2 CH, 10 CH_2), 0.87 (*d*, $J \approx 6.5$ Hz; 3H, CH_3), 0.83–0.79 (*m*; 9H, 3 CH_3). **^{13}C NMR** (100 MHz, $CDCl_3$): δ (ppm) = 164.87, 164.36 (2*s*; 2 COO), 163.85, 156.96, 155.31, 144.22, 127.07, 120.99 (6*s*; 6 Ar–C), 132.44, 131.76, 122.39, 122.07, 115.14, 114.44 (6*d*; 6 Ar–CH), 68.41, 66.76 (2*t*; 2 OCH_2), 39.28, 37.32, 36.25, 34.95, 31.83, 29.35, 29.11, 26.01, 25.48, 24.72 (10*t*; 10 CH_2), 29.87, 28.00 (2*d*; 2 CH), 22.68, 22.64, 19.68, 14.13 (4*q*; 4 CH_3). **$C_{38}H_{50}O_6$ (602.80):** full MS ESI (electrospray ionization) (+) [50.00–1000.00]: 603 (100) $[M+H]^+$, 353 (45) $[M^+ - C_{16}H_{26}O_2]$, 233 (112) $[M+ - C_{16}H_{26}O_2 - C_7H_4O_2]$, 121 (5) $[M+ - C_{16}H_{26}O_2 - C_7H_4O_2 - C_8H_{16}]$.

Results and discussion

The mesomorphic properties of 4-[4-((*S*)-3,7-dimethyloctyloxy)phenoxy) carbonyl]phenyl 4-(*n*-octyloxy)benzoate (*DPCPB*)

The liquid crystalline properties of *DPCPB* were investigated by using a Mettler FP-82 HT hot stage and control unit in conjunction with a Leica DM2700P polarizing microscope. DSC thermograms of *DPCPB* were recorded on a PerkinElmer DSC-6, heating and cooling rate: 10 °C min^{-1} in a nitrogen atmosphere. The mesomorphic properties of DPCPB are given in Table 1.

DPCPB exhibits an enantiotropic non-tilted smectic mesophase (SmA) with a typical fan-shaped texture in non-treated microscopic glass slides and the focal conic texture in a 5-μm PI non-coated ITO cell providing planar alignment

Table 1 Mesophase, phase transition temperatures (°C) and the corresponding transition enthalpies (kJ/mol) of the compound DPCPB

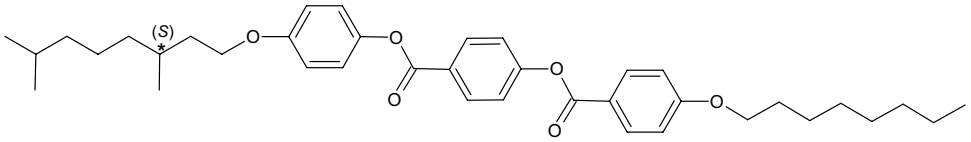

7

Compound	*T*/°C [Δ*H* kJ/mol][a]
DPCPB	**H**→: Cr 60.98 [*21.55*] SmA 139.64 [*2.23*] Iso Cr 32.69 [*1.98*] SmA 140.35 [*4.27*] Iso:←**C**

Cr crystalline, *SmA* non-tilted smectic mesophase, *Iso* isotropic liquid phase

[a]PerkinElmer DSC-6; enthalpy values in italics in brackets taken from the 2nd heating and cooling scans at a rate of 10 °C min^{-1}

as given in Fig. 1a,b. The focal conic texture in the homeotropically alignment sample between ordinary glassplates after shearing (Fig. 1c) was also appeared, and then, there is no observation of schlieren regions after relaxation time. The mesophase was detected by two calorimetric peaks at 60.98 °C and 139.64 °C in the DSC 2nd heating scans (see Fig. 2). The transition from SmA phase to crystalline was detected at 32.69 °C in DSC cooling thermogram.

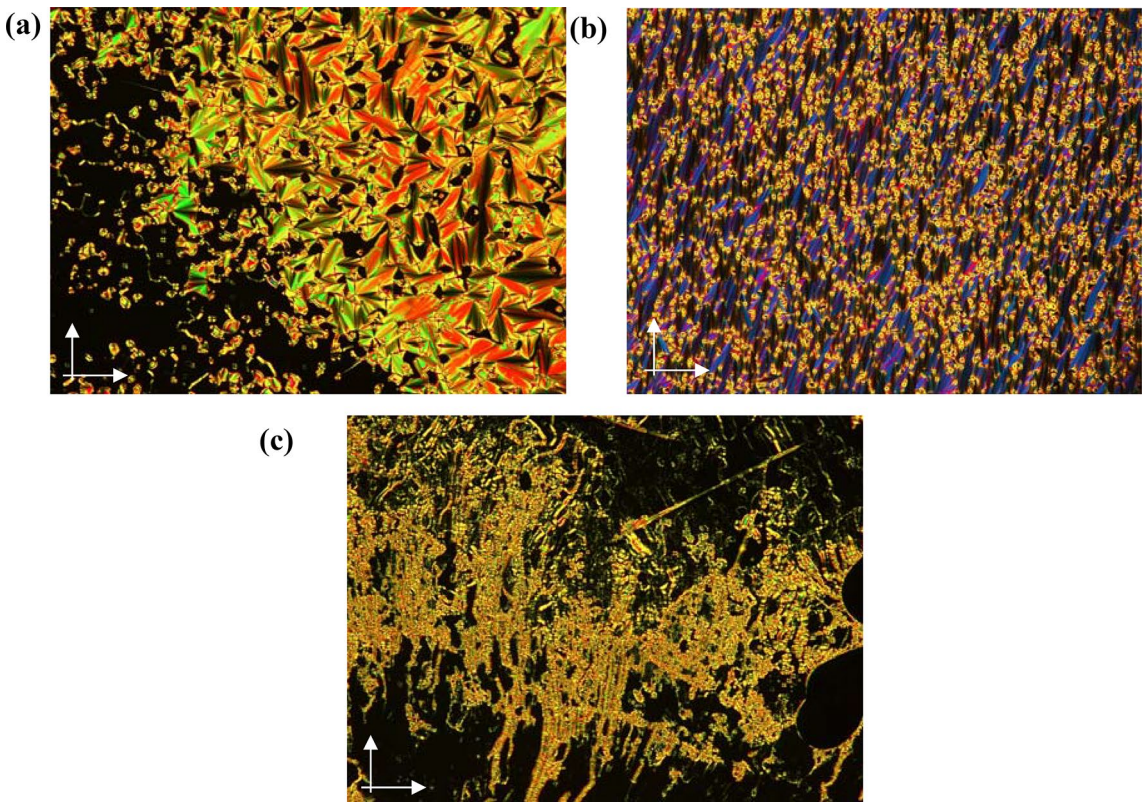

Fig. 1 Optical textures of mesophases of compound DPCPB observed between crossed polarizers (indicated by arrows) at 109.0 °C on cooling **a** The fan-shaped texture of the SmA phase between non-treated microscopic glass slides. **b** The appearance of focal conic texture in SmA phase in a 5-μm PI non-coated ITO cell providing planar alignment. **c** The focal conic texture of the SmA phase in the homeotropically alignment sample between microscopic glass slides after shearing (magnification 100×)

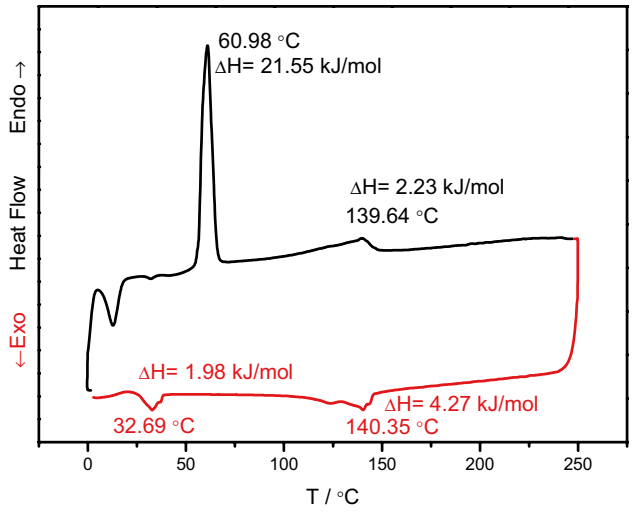

Fig. 2 DSC thermograms of compound DPCPB on 2nd heating and cooling (10 °C min^{-1})

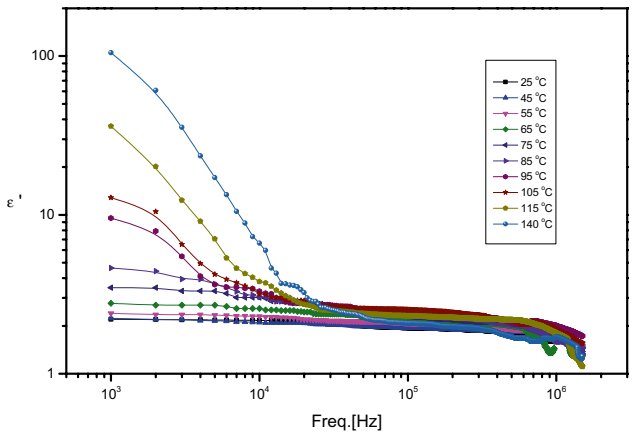

Fig. 3 The frequency variation of **a** the real part of the dielectric constant of DPCPB at different temperatures

Dielectric properties of 4-[4-((*S*)-3,7-dimethyloctyloxy)phenoxy) carbonyl]phenyl 4-(*n*-octyloxy)benzoate (*DPCPB*)

Dielectric constant or permittivity is a parameter of how easily a material is polarized by an electric field. Besides this, the dielectric constant (electrical permeability) shows how much energy is stored in the material in the presence of external electric field and how much energy is lost in the material. Here, the real (storage) component of dielectric constant ($\varepsilon'(\omega)$) indicates the amount of energy that can be stored in the dielectric material. The loss (imaginary) component of the dielectric constant ($\varepsilon''(\omega)$) is the measure of the energy emitted as heat in the dielectric material. Real

Table 2 Absorption coefficient and relaxation time of DPCPB at room temperature

Adj. R^2	α	$\tau_o(s)$
0.99973	0.014	9.36359E−8

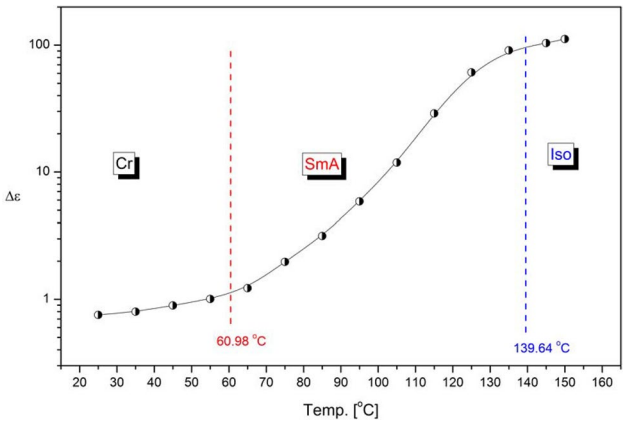

Fig. 4 Δε of DPCPB at different temperatures (frequency range: 1 k Hz to 1.5 M Hz)

component of dielectric constant ($\varepsilon'(\omega)$) depending on logarithmic angular frequency ($\omega = 2\pi f$) is given in Fig. 3.

The complex dielectric constant ($\varepsilon^*(\omega)$) consists of real $\left(\varepsilon'(\omega)\right)$ and imaginary ($\varepsilon''(\omega)$) components of dielectric constant, and $\varepsilon^*(\omega)$ can be formulated by Eq (1) [54, 55]

$$\varepsilon^*(\omega) = \varepsilon'(\omega) - i\varepsilon''(\omega) \tag{1}$$

The real component of dielectric constant decreases with increasing of frequency (Fig. 3).

The frequency dependence of the real dielectric constant $\varepsilon'(\omega)$ is described by Cole–Cole Eq. (2) [56].

$$\varepsilon'(\omega) = \varepsilon_\infty + \left(\varepsilon_s - \varepsilon_\infty\right)\frac{1 + \left(\omega\tau_0\right)^{1-\alpha}\sin\frac{1}{2}\alpha\pi}{1 + 2\left(\omega\tau_0\right)^{1-\alpha}\sin\frac{1}{2}\alpha\pi + \left(\omega\tau_0\right)^{2(1-\alpha)}} \tag{2}$$

τ_0 and α also represent relaxation time and absorption coefficient, respectively.

As shown in Fig. 3, the real component of dielectric constant increases with increasing of temperature at low frequency. As the frequency increases, the dielectric constant is almost constant for all temperatures with the (1–500 kHz) frequency range. The real component of the dielectric constant starts sharply increasing at 140° C, depending on the isotropic phase transition temperature.

The dielectric strength ($\Delta\varepsilon_s$) has been calculated as the difference between the low-frequency dielectric constant (ε_s) and high-frequency dielectric constant (ε_∞).

$$\Delta\varepsilon_s = \varepsilon_s - \varepsilon_\infty \tag{3}$$

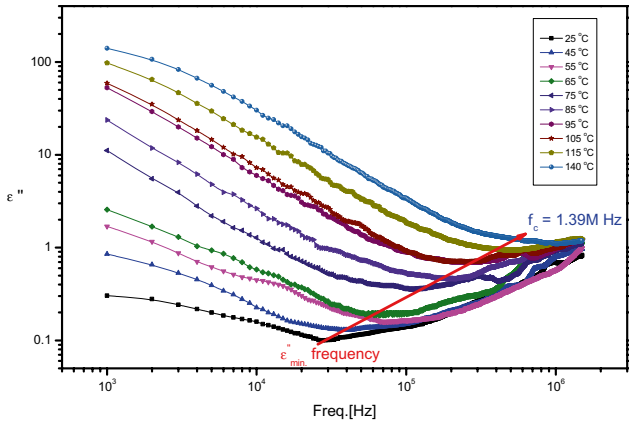

Fig. 5 The frequency variation of the imaginary parts of the dielectric constant of DPCPB at different temperatures

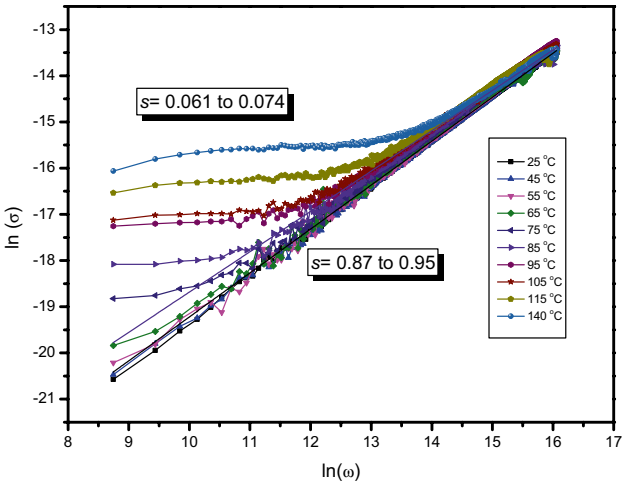

Fig. 6 The ln(σ) versus ln(ω) plots of DPCPB at different temperatures

Absorption coefficient (α) and relaxation times (τ) parameters have also been fitted by OriginPro 2015 graphic program in terms of Cole–Cole Eq. (2) on the frequency dependency of the relative dielectric constant ($\varepsilon' - f$) curves. Absorption coefficient takes values between zero and one. If absorption coefficient (α) is zero, Debye-type relaxation occurs for polar dielectrics. If absorption coefficient (α) is between zero and one that leads to the result of non-Debye-type relaxation [56]. The relaxation mechanism of DPCPB is nearly Debye type because α equals to 0.014 (Table 2).

Figure 4 shows dielectric strength ($\Delta\varepsilon$) values of DPCPB at different temperatures. Up to 65 °C, there is a slight change in dielectric strength due to the stability of the crystal structure. In the SmA phase, the dielectric strength increases logarithmically with increasing of temperature. In this SmA phase, the molecular dipoles of the liquid crystal are formed by increment of temperature, and because of this reason, the dielectric strength increases in the SmA phase. After 140 °C, the isotropic phase occurred.

Figure 5 shows imaginary component of dielectric constant. The absorption curve of the DPCPB shows a dielectric relaxation peak. The critic frequency, the imaginary component of dielectric constant decreases up to 1.39 MHz, after this value imaginary component of dielectric constant increases again because of decreasing oriented electrical molecular dipole effect in DPCPB. As the temperature increases, the minimum values of imaginary parts of dielectric constant are shifting toward the high frequency [57].

The imaginary component of dielectric constant decreases up to 10^5 Hz. After this value, it increases with increasing of frequency. As shown in Fig. 5, the maximum value of imaginary part of dielectric constant shown at 140 °C is related to the isotropic phase transition temperature. At high frequency, the imaginary parts of the dielectric constant of DPCPB are almost constant for all temperature.

Thanks to ln(σ) versus ln(ω) graph (Fig. 6), information about conductivity mechanism of DPCPB can be obtained. According to Jonscher's Universal Conductivity, power law obeys $\sigma = \sigma_{dc} + A\omega^s$. σ_{dc} is dc component, $A\omega^s$ is ac component and s parameter is frequency exponent [58, 59]. The frequency exponent can be calculated by the slope of ln(σ) versus ln(ω) graph (Fig. 6).

As shown in Fig. 6, up to 65 °C, s parameter varies from 0.87 to 0.95 and the conductivity mechanism is CBH (correlated barrier hoping) model because of $0 < s < 1$. As temperature increases, it occurs two conductivity mechanisms. At low angular frequency, the conductivity mechanism is nearly DC ($s = 0.061$ to 0.074), and at high angular frequency, the conductivity mechanism is CBH model ($s = 0.87$ to 0.95). One of the most famous and successful models put forward to explain the AC conduction mechanism in amorphous materials is the correlated barrier hopping (CBH) model by Elliott in 1987 [60, 61]. The theory was developed to explain the electrical transport in materials.

In CBH model thermally activated charge carriers hop between two localized sites over the potential barrier separating them. The temperature dependence of frequency exponent s is given $s = 1 - (6k_BT/W_m)$ and T is the temperature (K), W_m is the optical band gap (eV) of the material, and k_B is the Boltzmann constant (ev/K) [62, 63].

Conclusions

In this work, a new phenylbenzoate-based chiral calamitic liquid crystal DPCPB which composed of three aromatic rings with ester linking groups, *(S)-3,7-dimethyloctyloxy* chiral unit at one of terminals and *n*-octyloxy chain at the other

end has been synthesized and characterized. DPCPB exhibits an enantiotropic non-tilted smectic mesophase (SmA) with a typical fan-shaped texture in a wide temperature range. According to variation of real component of dielectric constant depending on frequency, the real component of dielectric constant increases sharply at 140 °C which is related to the isotropic phase transition temperature. The relaxation mechanism of DPCPB is nearly Debye type. Up to 65 °C the conductivity mechanism is correlated barrier hoping (CBH), and after this temperature, the conductivity mechanism is nearly DC. In this study, the determination of dielectric parameters clearly enables the verification of the phase transition temperatures of DPCPB which were determined both DSC and POM techniques. The dielectric investigation is of significant interest as a complementary method for the full characterization of thermal as well as electro-optic behavior of LCs used in technological applications.

Acknowledgements This research has been supported by Yildiz Technical University Scientific Research Projects Coordination Department with the Projects No.: 2015-01-02-YL04.

References

1. J.W. Goodby, P.J. Collings, T. Kato, C. Tschierske, H. Gleeson, P. Raynes, *Handbook of Liquid Crystals: Fundamentals*, vol. 1 (Wiley, Weinheim, 2014)
2. P.J. Collings, M. Hird, *Introduction to Liquid Crystals Chemistry and Physics* (Taylor and Francis Ltd., London, 1997)
3. T. Kato, N. Mizoshita, K. Kishimoto, Angew. Chem. Int. Ed. **45**, 38 (2006)
4. J.P.F. Lagerwall, G. Scalia, Curr. Appl. Phys. **12**, 1387 (2012)
5. K. Pal, M. Abd Elkodous, M.L.N. Madhu Mohan, J. Mater. Sci. Mater. Electron. **29**, 10301 (2018)
6. C.-J. Yun, J.-K. Song, J. INF. DISP. **18**(3), 119 (2017)
7. K. Pal, X. Yang, M.L.N. Madhu Mohan, R. Schirhagl, G. Wang, Mater. Lett. **169**, 37 (2016)
8. K. Pal, S. Thomas, M.L.N. Madhu Mohan, J. Nanosci. Nanotechnol. **17**(4), 2401 (2017)
9. J. De, W.-Y. Yang, I. Bala, S. Prasad Gupta, R.A. Kumar Yadav, D. Kumar Dubey, A. Chowdhury, J.-H. Jou, S. KumarPal, ACS Appl. Mater. Interfaces **11**, 8291 (2019)
10. V.S. Sharma, A.P. Shah, A.S. Sharma, M. Athar, New J. Chem. **43**, 1910 (2019)
11. J. De, S. Prasad Gupta, S. Sudheendran Swayamprabha, D. Kumar Dubey, I. Bala, I. Sarkar, G. Dey, J.-H. Jou, S. Ghosh, S. Kumar Pal, J. Phys. Chem. C **122**, 23659 (2018)
12. A. Kumar Yadav, B. Pradhan, H. Ulla, S. Nath, J. De, S. Kumar Pal, M.N. Satyanarayan, A.S. Achalkumar, J. Mater. Chem. C **5**, 9345 (2017)
13. E. Oton, J.M. Oton, M. Cano-Garcia, J.M. Escolano, X. Quintana, M.A. Geday, Opt. Express **27**(7), 10098 (2019)
14. R. Nandi, L. Loitongbam, J. De, V. Jain, S. Kumar Pal, Analyst **144**, 1110 (2019)
15. P. Popov, E.K. Mann, A. Jákli, J. Mater. Chem. B **5**, 5061 (2017)
16. H.K. Bisoyi, Q. Li, Prog. Mater. Sci. **104**, 1 (2019)
17. K. Pal, U. Narayan Maiti, T. Pal Majumder, S. Chandra Debnath, S. Ghosh, S. Kumar Roy, J. Manuel Oton, Nanotechnology **24**, 125702 (2013)
18. K. Pal, M.L.N. Madhu Mohan, B. Zhana, G. Wang, J. Mater. Chem. C **3**, 11907 (2015)
19. B. Donnio, D. Guillon, R. Deschenaux, D.W. Bruce, in *Comprehensive Coordination Chemistry II*, ed. by J.A. McCleverty, T.J. Meyer (Elsevier, Oxford, 2003)
20. S.A. Hudson, P.M. Maitlis, Chem. Rev. **93**, 861 (1993)
21. N. Hoshino, K. Takahashi, T. Sekiuchi, H. Tanaka, Y. Matsunaga, Inorg. Chem. **37**, 882–889 (1998)
22. N. Hoshino, Coord. Chem. Rev. **174**, 77 (1998)
23. M. Hagar, H.A. Ahmed, G.R. Saad, J. Mol. Liq. **273**, 266 (2019)
24. X. Kong, B. Zhong Tang, Chem. Mater. **10**, 3352 (1998)
25. A.M. El Defrawy, S.Z. Mohammady, M.G. Elghalban, H.F. El-Sharief, Orient. J. Chem. **33**(3), 1190 (2017)
26. G. Hegde, G. Shanker, S.M. Ganc, A.R. Yuvaraj, S. Mahmood, U. KumarMandal, Liq. Cryst. **43**(11), 1578 (2016)
27. H.T.A. Wilderbeek, M.G.M. van der Meer, M.A.G. Jansen, L. Nelissen, H.R. Fischer, J.J.G.S. van Es, C.W.M. Bastiaansen, J. Lub, D.J. Broer, Liq. Cryst. **30**(1), 93 (2003)
28. O.V. Potemkina, S.A. Kuvshinova, O.I. Koifman, Russ. J. Gen. Chem. **89**(3), 597 (2019)
29. R.B. Meyer, L. Liebert, L. Strzelecki, P. Keller, J. Phys. Lett. **36**, 69 (1975)
30. M. Hird, Liq. Cryst. **38**, 1467 (2011)
31. J.W. Goodby, R. Blinc, N.A. Clark, S.T. Lagerwall, M.A. Osipov, S.A. Pikin, T. Sakurai, K. Yoshino, B. Zenks, *Ferroelectric Liquid Crystals. Principle and Applications* (Gordon and Breach, Philadelphia, 1991)
32. R.P. Lemieux, Acc. Chem. Res. **34**(11), 845 (2001)
33. S.P. Sreenilayam, D. Rodriguez-Lojo, D.M. Agra-Kooijman, J.K. Vij, V.P. Panov, A. Panov, M.R. Fisch, S. Kumar, P.J. Stevenson, Phys. Rev. Mater. **2**, 025603 (2018)
34. C.V. Yelamaggad, G. Shanker, U.S. Hiremath, S. Krishna Prasad, J. Mater. Chem. **18**, 2927 (2008)
35. G. Karanlık, H. Ocak, B. Bilgin-Eran, J. Mol. Liq. **275**, 567 (2019)
36. H. Ocak, B. Bilgin-Eran, C. Tschierske, U. Baumeister, G. Pelzl, J. Mater. Chem. **19**, 6995–7001 (2009)
37. H.-S. Kitzerow, C. Bahr (eds.), *Chirality in Liquid Crystals* (Springer, New York, 2001)
38. J.P.F. Lagerwall, F. Giesselmann, ChemPhysChem **7**, 20 (2006)
39. A. KatariyaJain, R.R. Deshmukh, Liq. Cryst. **46**(8), 1191 (2019)
40. E. Ahlatcıoğlu Özerol, H. Ocak, ChemistrySelect **4**, 9006 (2019)
41. B. Barman, B. Das, M.K. Das, V. Hamplova, A. Bubnov, J. Mol. Liq. **283**, 472 (2019)
42. A. Sharma, P. Malik, R. Dhar, P. Kumar, Bull. Mater. Sci. **42**, 215 (2019)
43. K. Agrahari, T. Vimal, A. Rastogi, K. Kumar Pandey, S. Gupta, K. Kurp, R. Manohar, Mater. Chem. Phys. **237**, 121851 (2019)
44. A. Kumar Misra, P. Kumar Tripathi, K. Kumar Pandey, F. Pati Pandey, S. Singh, A. Singh, Mater. Res. Express **6**, 1050d2 (2019)
45. L. Jongen, B. Goderis, I. Dolbynya, I. Binnemans, Chem. Mater. **15**, 212 (2003)
46. S. Uma Hiremath, Tetrahedron **70**(32), 4745 (2014)
47. P.C. Jocelyn, N. Polgar, J. Chem. Soc. (Resumed) **0**, 132 (1953)
48. D. Güzeller, H. Ocak, B. Bilgin-Eran, M. Prehm, C. Tschierske, J. Mater. Chem. C **3**, 4269 (2015)
49. H. Kondo, T. Okazaki, N. Endo, S. Mihashi, A. Yamaguchi, H. Tsuruta, S. Akutagawa, Jpn. Kokai Tokkyo Koho, JP 63033351 A 19880213 (1988)
50. E. Chin, J.W. Goodby, Mol. Cryst. Liq. Cryst. **141**, 311 (1986)
51. S.-C. Kuo, K.-H. Lee, L.-J. Huang, L.-C. Chou, T.-S. Wu, T.-D. Way, J.-G. Chung, J.-S. Yang, C.-H. Huang, M.-T. Tsai, PCT Int. Appl., WO 2012009519 A1 20120119 (2012)
52. C. Tschierske, H. Zaschke, J. Prakt. Chem. **331**, 365 (1989)
53. S. Karavelioglu, Kiral Kalamitik Molekül Geometrili Mesogenik Materyallerin Sentezi ve Karakterizasyonu. M.Sc. Thesis, Yıldız Technical University, Istanbul (2016)

54. P.R.G. Fernandes, K.A. da Silva, H. Mukai, E.C. Muniz, J. Mol. Liq. **229**, 319 (2017)
55. B. Korkmaz, E. Ahlatcıoğlu Özerol, Y. Gürsel, B.F. Şenkal, M. Okutan, J. Mol. Liq. **266**, 132 (2018)
56. K.S. Cole, R.H. Cole, J. Chem. Phys. **9**, 341 (1941)
57. N.Y. Canli, H. Ocak, A. Yildiz, M. Okutan, B.B. Eran, J. Mol. Liq. **238**, 370 (2017)
58. A.K. Jonscher, *The Universal Dielectric Response: A Review of Data Their New Interpretation* (Chelsea Dielectric Group, London, 1978)
59. E. Ahlatcıoğlu Özerol, Polym. Bull. **76**(10), 5301 (2019)
60. S.R. Elliott, Adv. Phys. **36**, 135 (1987)
61. M. Okutan, O. Köysal, S.E. San, E. Şentürk, J. Non-Cryst. Solids **355**, 2674 (2009)
62. H.A.M. Ali, M.A. Ibrahim, Mater. Sci. **34**(2), 386 (2016)
63. A. Yildiz, N.Y. Canli, Z.G. Özdemir, H. Ocak, B.B. Eran, M. Okutan, Phys. B **485**, 21 (2016)